JOURNAL OF MATERIALS SCIENCE 20 (1985) 1480–1493

Friction and wear of amorphous Ni–B, Ni–P films obtained by ion implantation into nickel

J. TAKADOUM, J. C. PIVIN, J. CHAUMONT
CSNSM, BPI, 91406 Orsay Cedex, France

C. ROQUE-CARMES
Laboratoire de Microanalyse des Surfaces, ENSMM, 25030 Besancon Cedex, France

The wear and friction resistance of nickel surfaces implanted with increasing doses of boron or phosphorous was investigated, with a pin-on-disc geometry and a 100C6 steel rider, in air. The seizure resistance is drastically improved when the implanted dose is sufficiently high to give an amorphous Ni–B or Ni–P layer.

1. Introduction

The physical and mechanical properties of metallic glasses have been the object of great interest during the last decade [1–4], because they must be inherently different from those of crystalline metals and they already have applications in the aerospace or electronic industries [5].

Metallic glasses generally exhibit high ductility combined with high strength at temperatures below the temperature of crystallization [4, 6], and Ni–B brazed foils are used, for instance, in engine valves [5]. Fe–Ni–B glasses also are used as magnetic heads and tapes for video recorders [5], because of the combination of a high permeability with high hardness and wear resistance.

However, few studies [5–8] deal with the surface properties of metallic glasses, in spite of the important contribution of surface layers to all properties because of the small thickness of commonly available glasses. A problem encountered in fundamental studies is their heterogeneity of structure and compostion: crystallites at the surface, oxide inclusions in quenched ribbons and evaporation or sputtering deposits, gradients of composition in electroless or electrolytic deposits, and numerous additions to stabilize the amorphous structure in most of them [9, 10]. This hampers significant experiments on their intrinsic reactivity or friction behaviour. Moreover, the uneven profile of ribbons means that few reliable mechanical tests or wear experiments could be done until now [4].

It thus appears very interesting to study the surface properties of amorphous layers obtained by ion implantation. Numerous alloys can be obtained in the amorphous state [11–14] by implanting in pure metals ion doses such that the composition in the implanted layer corresponds to chemical criteria of glass stability. Note that novel alloys could be obtained in some cases [14], maybe because the disorder induced by the collision cascade is set in a time (10^{-12} sec) much shorter than the cooling time of materials quenched from the liquid or gas state (10^{-6} sec). Alloys of simple composition and free of impurities are obtained, provided that the ion beam is correctly mass-filtered and the vacuum in the sample chamber sufficiently clean. The kinetics of amorphization of nickel surfaces by boron or phosphorus implantation was previously established [13–15].

Now it is well established that ion implantation can improve the wear resistance and friction of materials for large sliding distances, in spite of the shallow thickness of the implanted layer [16–20]. The diffusion of the implanted atoms during friction (because of a momentary increase of the temperature at areas of contact and of high compressive stress) was invoked to explain that the beneficial effect of implantation endures long after

 0022–2461/85 $03.00 + .12

removing a thickness of material over 10 times the implanted depth. This diffusion was observed by nuclear reaction analysis on steels surfaces implanted with nitrogen [16].

On the other hand the decrease of wear rate was generally attributed to the segregation of atoms of boron, carbon, nitrogen, phosphorus, titanium, etc. on dislocations and to the formation of carbides, nitrides or other types of precipitates, both being factors which should induce hardening [19]. These arguments are satisfactory to explain a suppression of abrasion, but modification of the physicochemical properties of implanted surfaces has rather to be involved to explain a suppression of adhesion. Neither the reactivity of the surfaces (except for electrochemical tests) with the medium of wear tests, nor the segregation or precipitation of hardening particles were studied until now. In the case of amorphized layers the reactivity can be changed not only because of a modification of the composition but also to the structure: the surface energy of amorphous materials is less than that of crystalline ones, and thus the kinetics of oxygen or lubricant adsorption and of alloying with the surface of the counterpart materials must be much slower. Recent experments [20] on Ni–26% B–2% Si ribbons and nickel surfaces implanted with boron and phosphorus have shown that the kinetics of oxygen adsorption at room temperature or of mild oxidation at 150° C are much slower for amorphous surfaces than for surfaces annealed at temperatures above the crystallization threshold.

Note, however, that a crystallization of the surface during the sliding process was observed in some cases on Fe–B or Fe–Ni–B ribbons [5, 7].

We report here preliminary results on the wear resistance and dry friction of nickel surfaces implanted with boron or phosphorus. Experiments are on hand to characterize the hardness of implanted layers and their possible crystallization during friction.

2. Experimental details

2.1. Samples

The samples were discs of Ni 200 with the composition given in Table I. Their surfaces were polished with SiC papers and diamond pastes down to 1 μm, then electrolytically in a solution of composition 45% $CH_3COOH + HClO_3$ + 50% 2-butoxyethanol at 0° C, 20 V for 5 min. The average roughness of surfaces was 0.01 μm.

TABLE I Impurities content (ppm) in the Ni 200 ingot

C	S	Si	Al	Co	Cu	Fe	Mg	Mn	Ni
600	10	250	200	300	100	500	350	2000	bal.

Then surfaces were implanted in the machine built at the CSNSM Orsay [21]. Parameters of the implantation are given in Table II: R_p is the mean projected range of implanted ions, ΔR_p the straggling of the distribution, $C(R_p)$ the maximum of phosphorus or boron concentration at depth R_p.

Implantation profiles were characterized by SIMS and GDOS [22]: experimental values of projected ranges are in good agreement with calculated ones, but the distributions are sensibly wider than the theory predicts and thus concentrations $C(R_p)$ are lower than their calculated values (Table II). It was verified by diffraction of X-rays at grazing incidence [29] and by Rutherford back-scattering of energetic He^+ ions at channelling incidence on nickel single crystals that the nickel substrate is amorphous at depth R_p for a dose of 1.2×10^{17} P cm^{-2} or 2.5×10^{17} B cm^{-2}; the whole implanted layer is amorphous for a dose of 2.5×10^{17} P cm^{-2} or 4×10^{17} B cm^{-2}.

2.2. Wear experiments

The apparatus was of the type designed at INSA in Lyon [23] with a pin-on-disc configuation. The riders were spheres of 100 C6 steel with a diameter of 5 mm. A new rider was used for each test. The experiments were carried out in air, without lubrication, under applied loads, P, of 2.5 or 5.0 N, and with rotation speeds of 1.5 or 5.5 r.p.m. The track diameter being 31 mm, the sliding speeds were 146 mm or 536 mm min^{-1}.

The sample holder was modifed in order to ensure that the surface of the sample was perfectly horizontal and thus the load applied normally. The sample position was corrected by means of 3 screws at 120°, and it was checked with a displacement transducer: defects of horizontally were lower than ± 20 μm on surfaces of 25 cm^2 area.

Values of the tangential force resisting motion, F, measured by the strain gauge were calibrated before each test with standard weights.

2.3. Roughness measurements

Three-dimensional imagings of the topography of sliding tracks were recorded by a stylus technique (Talysurf 5 machine with a stylus radius of 2 μm).

TABLE II Implantation parameters

Ions	Energy (keV)	R_p (nm)	ΔR_p (nm)	doses (cm^{-2})	$C(R_p)$ theory	$C(R_p)$ experiment
B	50	61	23	1×10^{16}	1.9×10^{-2}	
				5×10^{16}	9.5×10^{-2}	
				1×10^{17}	1.9×10^{-1}	
				2×10^{17}	3.8×10^{-1}	
				3×10^{17}	5.7×10^{-1}	
B	70	95	44	8×10^{14}	0.8×10^{-3}	
				4×10^{15}	4.1×10^{-3}	3.1×10^{-3}
				2.2×10^{16}	2.2×10^{-2}	1.7×10^{-2}
				4.5×10^{16}	4.5×10^{-2}	3.4×10^{-2}
				1.2×10^{17}	1.2×10^{-1}	0.9×10^{-1}
				3.0×10^{17}	3.0×10^{-1}	2.2×10^{-1}
P	125	53	24	1×10^{15}	1.8×10^{-3}	1.1×10^{-3}
				1×10^{16}	1.8×10^{-2}	1.1×10^{-2}
				5×10^{16}	9.1×10^{-2}	5.5×10^{-2}
				1×10^{17}	1.8×10^{-1}	1.1×10^{-1}
				2.5×10^{17}	4.5×10^{-1}	2.1×10^{-1}

The surface height, z, in each point of the explored area of $3.6 \times 10^5\ \mu m^2$, was measured by successive scans along lines 600 μm long with identification steps x_i, y_j of 3 μm along each line and between successive lines (via stepping motors). For more details on this apparatus and on the determination of statistical parameters defining the distribution of asperity heights, $z(i, j)$ slopes, curvatures, and bearing areas, see [24, 25].

The useful parameters in the case of sliding tracks are the width of the track, l, its mean depth, d, and the worn volume per unit length of track, v. This last parameter was computed by the following procedure. The tracks exhibit ridges or peaks over the mean surface (see Figs. 6 to 9) due to the plastic deformation of the material during contact and to the adhesion of pin and disc surfaces at the end of the contact. Thus:

(i) for each scanned line y_j an unworn surface is defined by interpolating the line $z(x_i)$ defining the surface outside the strained area on both sides of the track,

(ii) then z values over this basic line and z values under this line are summed separately in order to calculate for each y_j the protruding volume $v+$ over the unworn surface and the volume $v-$ under this surface,

(iii) $v+$ and $v-$ are averaged over all y_j. $< v+ >$ gives an idea of the extent of plastic deformation and adhesion in the contact, while $(< v- > - < v+ >)$ gives the worn volume per unit length.

An additional processing of three-dimensional imagings of topographical defects was to deconvolute them into defects of low and high periodicity, in order to obtain, respectively, a smoothed image of the track shape and an image of the roughness outside and inside the track. This processing gives additional information on the wear mechanism.

The procedure used to image the smoothed surface is simply to average asperity heights over squares of 81 points $[x_i - 4, x_i + 4] \times [y_j - 4, y_j + 4]$ to calculate a value $< z(x_i, y_j) >$. The image of the roughness is given by the difference in each point of $z(x_i, y_j)$ and $< z(x_i, y_j) >$.

2.4. Surface analysis

The tracks were first observed by scanning electron microscopy (SEM), and secondary X-ray emission excited by the electron beam (EMA) was used to analyse the surface. Energy dispersion of X-rays with a Si(Li) cyrstal was preferred to wavelength dispersion because the surfaces of tracks are rough.

Secondary ion mass spectrometry and microscopy (SIMS) was used to analyse the depth composition of worn surfaces with high sensitivity and resolution. The machine used was a CAMECA SMI 300: details of its optics and on quantification of concentrations are given in [26, 27].

Depth profiles were recorded on areas 10 μm in diameter within each track. The primary ions of bombardment were Ar^+ of energy 5.5 keV. In some cases the surfaces were flooded with oxygen in order to form continuously a thin oxide film on the surface, in which the sputtering yield and ionization probability of atoms is more uniform than in surfaces free of oxygen [26]. Thus the

concentration of nickel, boron, phosphorus, iron and chronium at each depth could be quantified (elements in low concentration, namely carbon, silicon, aluminium and manganese, were neglected in the calculation of ionization probabilities and of concentrations from the model [27]). Sputtering rates were crudely estimated by recording depth profiles of the implanted element, boron or phosphorus, on areas outside the wear tracks. Such estimates neglect the variation of the sputtering yield with the composition of the surface: this varies by a factor 2 with the concentration of boron or phosphorus in films containing 0 to 20% of these elements. Moreover, the sputtering yield varies continuously with depth in the case of implanted layers of wear tracks. Note, however, that the influence of low concentrations of iron, chromium, manganese, carbon etc. on the sputtering yield can be neglected.

Profiles were also recorded on surfaces free of adsorbed oxygen, in order to study the depth distribution of this element in wear tracks. In such conditions of analysis, the ionization probabilities of atoms are strongly dependent on their chemical environment: in particular the ionization probabilities of metal ions such as Ni^+, Fe^+, Cr^+ vary by several orders of magnitude with the oxygen concentration. Such profiles permit only qualitative comparisons of:

(a) the depth distributions of boron or phosphorus in order to reveal their possible diffusion during the wear process;

(b) the amounts of oxygen, carbon, iron, chromium, manganese, silicon, aluminum and other contaminants and the thickness of layers containing them, in order to determine whether some material is transferred from the pin to the disc or these atoms diffuse inside the disc surface during the time of contact.

3. Experimental results

3.1. Friction

Figs. 1 and 2 show typical evolutions of the friction coefficient, μ, as a function of the sliding distance, for various doses of boron and phosphorus implanted into nickel. In the case of pure nickel some seizures ($\mu > 1$) are observed after a few minutes only of wear. Between successives seizures μ is of the order of 0.7. For surfaces implanted with boron or phosphorus the initial value of μ is about 0.2. The first seizure is observed after times increasing with the boron or phosphorus

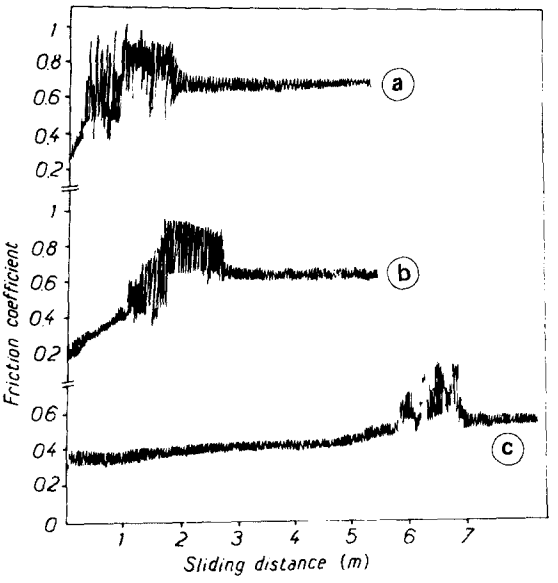

Figure 1 Variation of the friction coefficient with the sliding distance under an applied load of 5 N and with a rotation speed of 5.5 r.p.m. for nickel surfaces implanted with various doses of 50 keV boron ions: (a) 5×10^{16} cm^{-2}, (b) 10^{17} cm^{-2}, (c) 3×10^{17} cm^{-2}.

dose. Figs. 3 to 5 show the variation of the sliding distance before seizure with the implanted dose, for the different charges and sliding velocities. For doses over 1×10^{17} phosphorus or 2×10^{17} boron (near the limit of complete amorphicity at R_p) no seizure was observed after sliding several metres

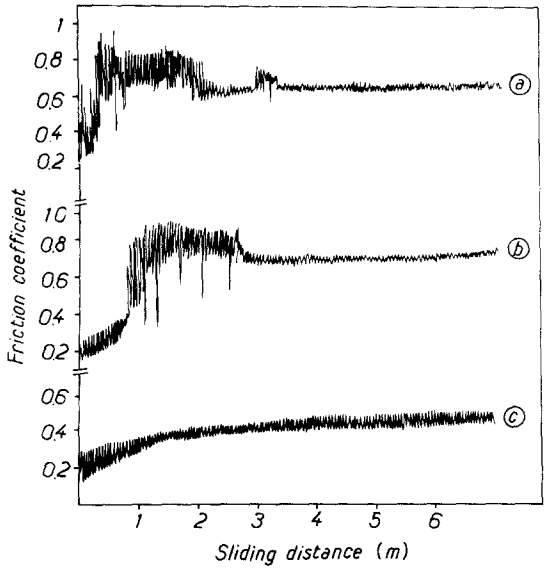

Figure 2 As Fig. 1 for nickel surfaces implanted with 125 keV phosphorus ions: (a) 10^{15} cm^{-2}, (b) 5×10^{16} cm^{-2}, (c) 2.5×10^{17} cm^{-2}.

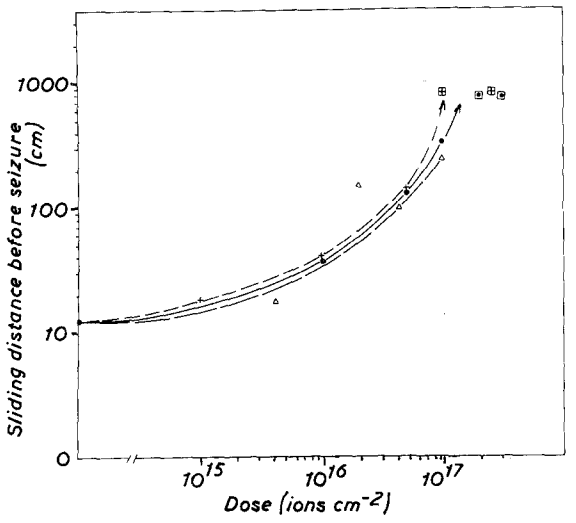

Figure 3 Variation of the sliding distance before seizure with the implanted dose of —●— 50 keV boron, — —△— — 70 keV boron, — —+— — 125 keV phosphorus. The applied load was 2.5 N and the rotation speed 1.5 r.p.m. The framed symbols correspond to tests during which no seizure occurred after 10 m sliding.

and μ values remained ~ 0.4 (cf. Figs. 3 to 5). Note that phosphorus implantation gives to nickel a better friction resistance than does boron at comparable concentration and implantation depth.

3.2. Wear

Examples of three-dimensional recordings of the track topography are given in Figs. 6 to 9. It appears first that the wear mechanism is very different for pure nickel or nickel implanted with low doses of boron or phosphorus and for a amorphous layers:

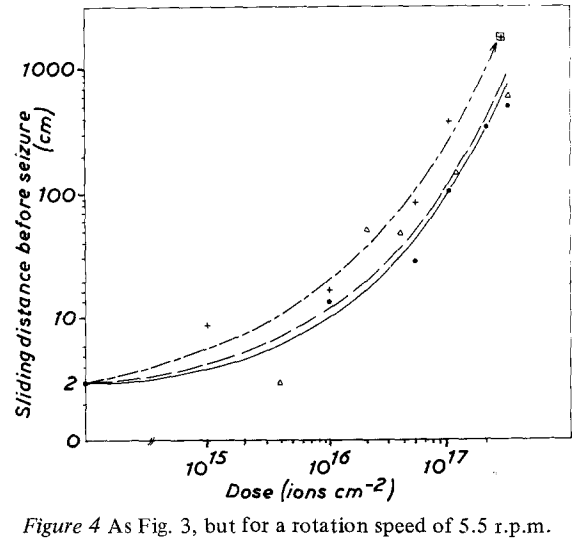

Figure 4 As Fig. 3, but for a rotation speed of 5.5 r.p.m.

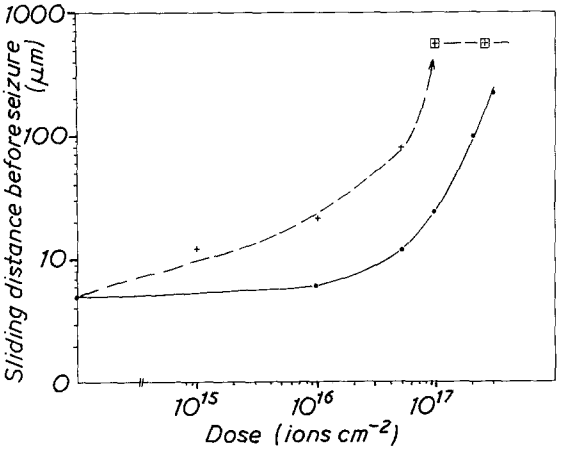

Figure 5 As Fig. 3 but for an applied load of 5 N.

1. in the first case, the topography indicates that adhesion occurred between pin and disc surfaces. The smoothed profiles exhibit hills and valleys statistically distributed over the whole area of the track. Wear debris are also observed by optical microscopy or SEM,

2. in the second case, little debris is observed and the topography is characteristic of mild abrasive wear. The smoothed profiles exhibit continuous ridges along the boundaries of the tracks, and sometimes inside them. These ridges indicate that the plastic deformation of the surface during the contact is quite substantial. Note that they are not observed in the case of a thick Ni–26% B electroless coating worn under the same conditions (Fig. 9c).

It is well known that the plastic deformation of a thin layer by identation is affected by the mechanical properties of the substrate [28]: hard materials deposited on soft substrates appears the softer, the thinner the deposit, while the apparent hardness of soft deposits on hard substrates increases as their thickness decreases. The mechanical properties of implanted layers are thus not really characteristic of their intrinsic composition and structure, but of those of a composite material.

Otherwise, the residual roughness (after subtraction of the smoothed relief) is much greater in the tracks than outside the track but quite independant of the implanted dose.

The variation of the track width, l, for identical sliding distances, with the implanted dose (Figs. 10 and 11) indicates an abrupt decrease of the wear kinetics at the critical dose for amorphization.

Values of the worn volume per unit length

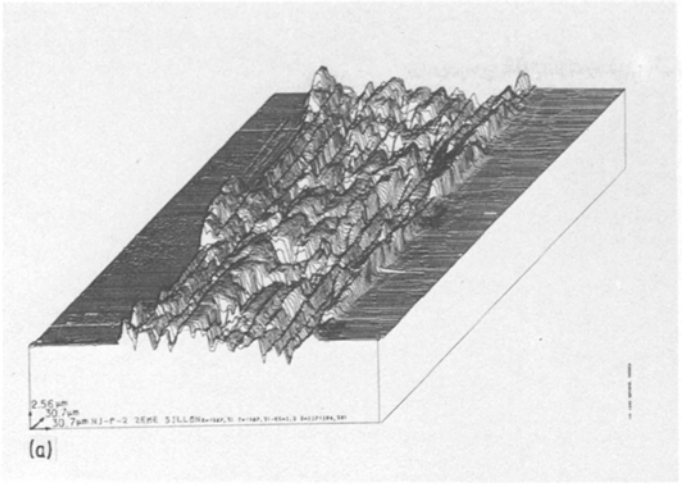

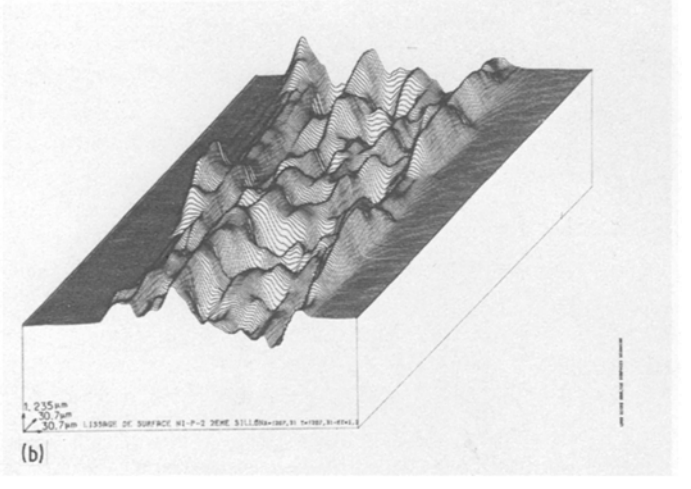

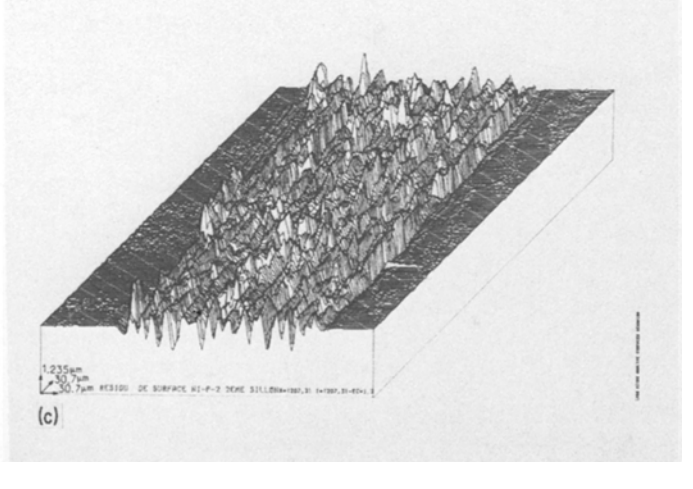

Figure 6 Topography of the track in nickel surface implanted with 5×10^{15} phosphorus ions of energy 125 keV, after sliding 7 m under an applied charge of 5 N and at a speed of 1.5 r.p.m. (a) raw recording, (b) smoothed profile, (c) residual roughness. The depth scales are different for (a), (b), (c).

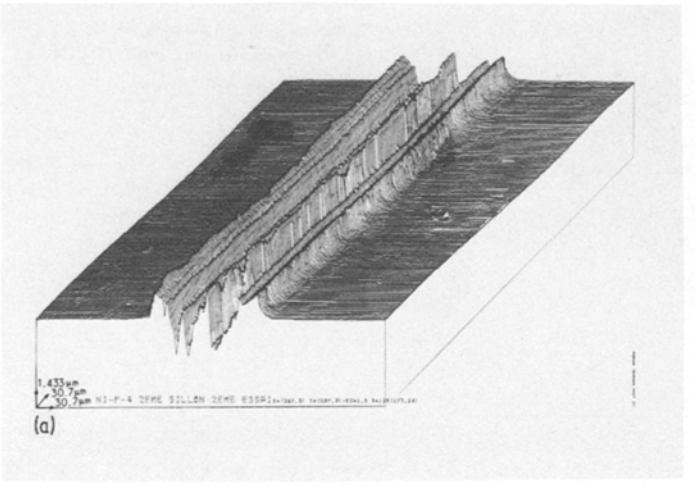

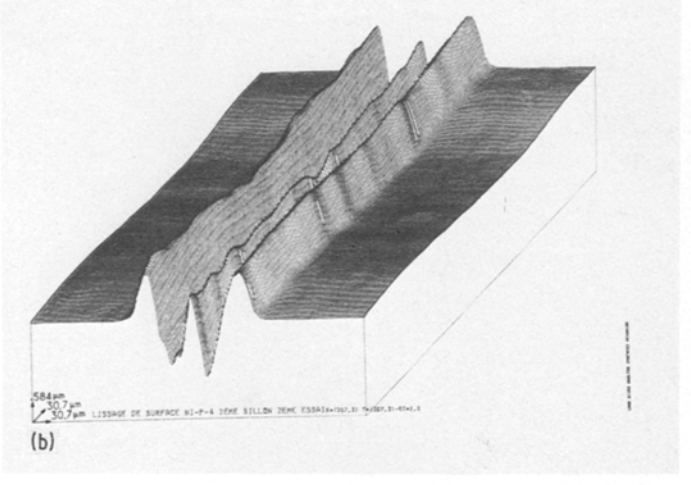

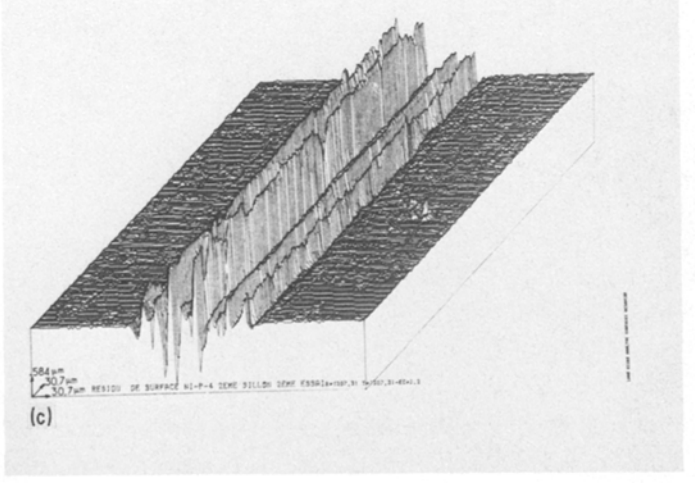

Figure 7 As Fig. 6, but for a surface implanted with 10^{17} phosphorus ions of energy 125 keV (dose near the limit of complete amorphicity).

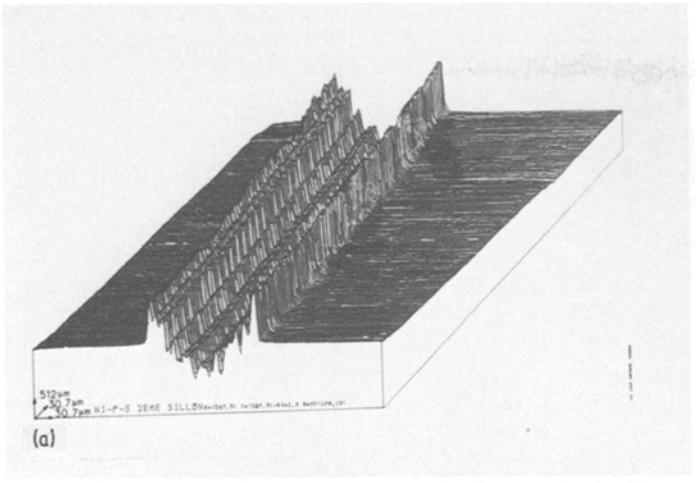

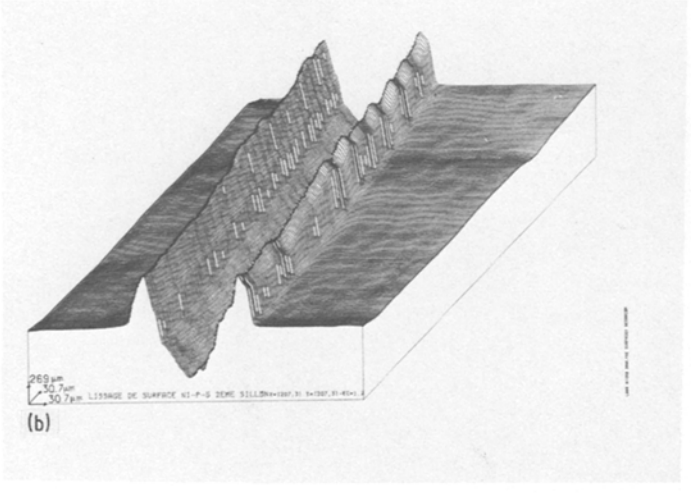

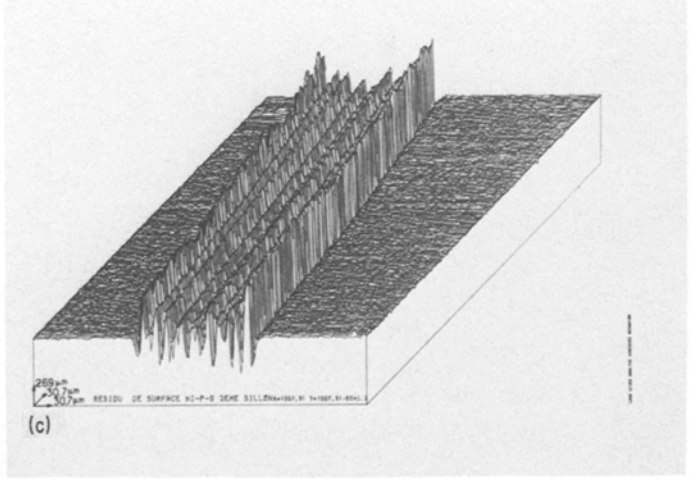

Figure 8 As Fig. 6, but for a surface implanted with 2.5×10^{17} phosphorus ions of energy 125 keV (dose over the limit of complete amorphicity).

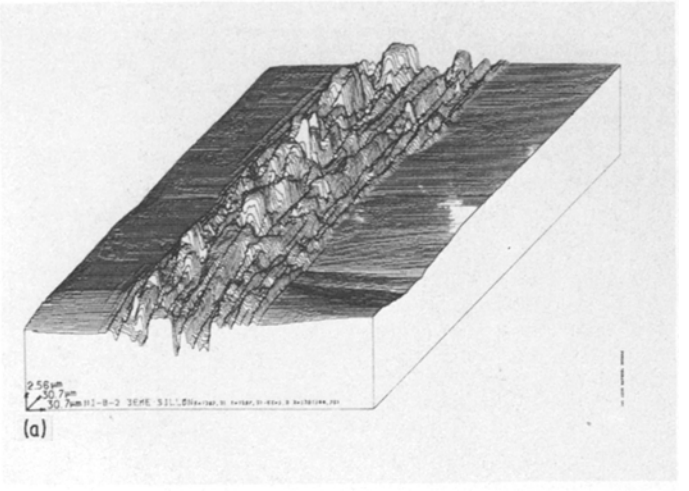

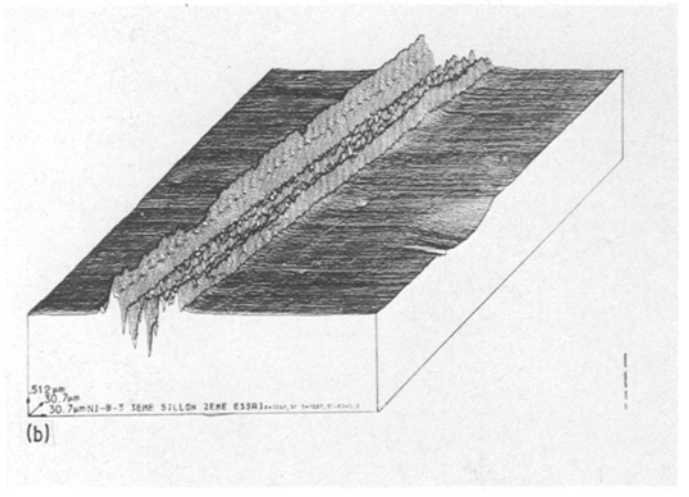

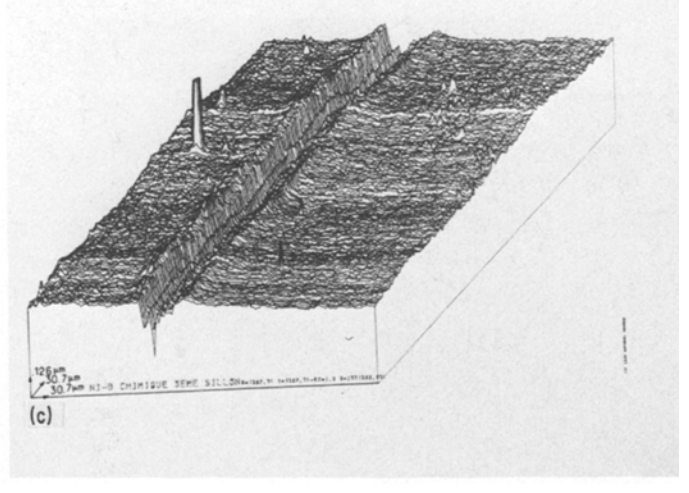

Figure 9 Raw recordings of the topography of tracks after sliding 12 m under an applied load of 2.5 N and at a speed of 1.5 r.p.m. for: nickel implanted with (a) 10^{16} B cm^{-2} of energy 50 keV, (b) 10^{17} B cm^{-2}, (c) Ni–26% B electroless coating (the peak on the left is a dust grain).

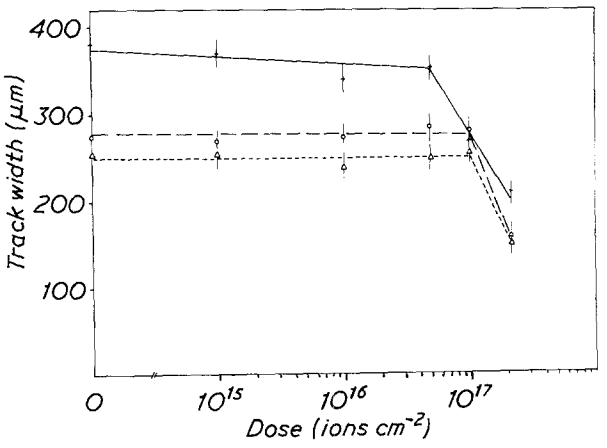

Figure 10 Variation of the track width with the dose of 125 keV phosphorus ions implanted into nickel for the following wear conditions: —+— 5 N, 1.5 r.p.m. ——o—— 2.5 N, 5.5 r.p.m. ——△—— 2.5 N, 1.5 r.p.m. The sliding distance was 7 m in all cases.

($< v- > - < v+ >$) are not very significant because in all cases volumes under the surfaces $< v- >$ and the protuding one $< v+ >$ are of the same order of magnitude (Table III). The measurement of the worn volume would require study of the whole track (10 cm long) in order to take into account displacements of matter in front of the pin and average the local variation of the deformations during contact and separation of the surfaces. However, the respective values of $< v- >$ and $< v+ >$ give qualitatively and idea of the extent of the wear and of the plastic deformation as a function of the implanted dose. Similarly to the track width they diminish abruptly at the critical dose for amorphization.

3.3. Transfer and diffusion during contact

In the case of severe wear, particles enriched in iron, chromium and oxygen were detected in the tracks by EMA. Material of the disc is also transferred to the pin behind the scarred area (Fig. 12 – the direction of rotation was marked when removing the pin of the tribometer).

SIMS profiles were recorded in wear tracks after removal of wear debris in order to study the diffusion of the implanted element and of atoms from the pin (Fig. 13.).

Iron, chromium, manganese, carbon, oxygen and the implanted species diffuse during the wear process. The thickness of diffusion films may be estimated approximately by comparison of sputtering times of films with that corresponding to the projected range of phosphorus or boron in unworn surfaces. They are of the order of 1 μm for surfaces implanted with low doses of boron or phosphorus and only 100 nm for nickel implanted with 2.5×10^{17} P cm^{-2}. In this last case most of the implanted dose remains in the track after

TABLE III

Samples	Wear conditions	$v+$ (μm^2)	$v-$ (μm^2)	$v- - v+$ (μm^2)
Ni + 10^{15} P	1.5 r.p.m.	338	429	91
Ni + 10^{16} P	500 g–7 m	330, 359	423, 328	93, – 31
Ni + 5×10^{16} P	500 g–7 m	312	399	87
Ni + 10^{17} P	500 g–7 m	–	–	–
Ni + 2.5×10^{17}	500 g–7 m	96	64	– 32
Ni + 10^{15} P	1.5 r.p.m.	379	128	– 251
Ni + 10^{16} P	250 g–7 m	242	248	5
Ni + 5×10^{16} P	250 g–7 m	267	243	25
Ni + 10^{17} P	250 g–7 m	151, 144	112, 122	– 39, – 22
Ni + 2.5×10^{17} P	250 g–7 m	66	52	– 14
Ni + 10^{16} B	1.5 r.p.m.	216	220	4
Ni + 5×10^{16} B	250 g–12 m	208	159	– 50
Ni + 10^{17} B	250 g–12 m	242	127	– 115
Ni + 2×10^{17} B	250 g–12 m	47	31	– 16
Ni + 3×10^{17} B	250 g–12 m	37, 50	15, 31	– 22, – 19
Ni–26% B electroless coating	250 g–12 m	8	9	1

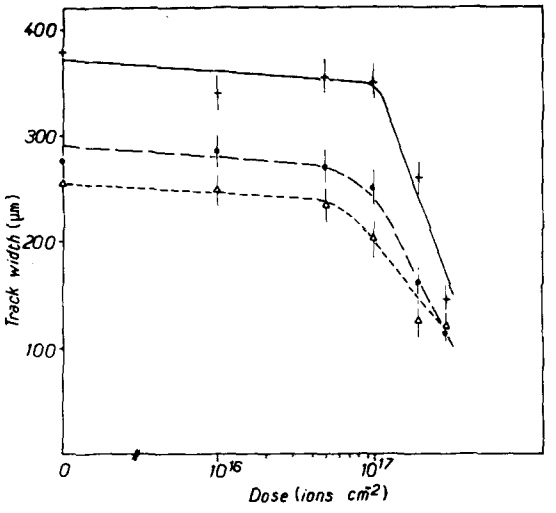

Figure 11 As Fig. 10, but for surfaces implanted with 50 keV boron ions.

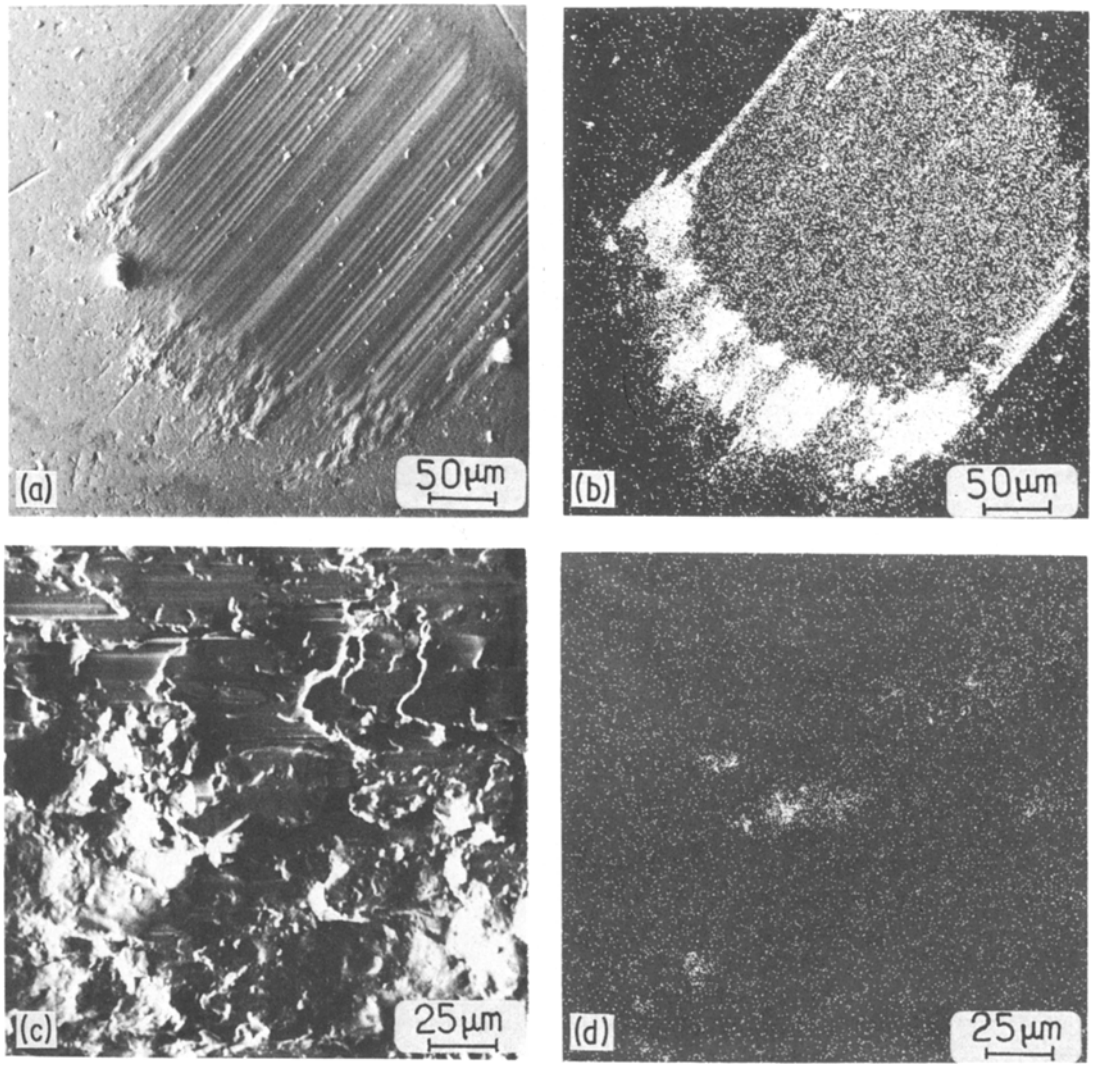

Figure 12 Electron microprobe analysis of pin and disc surfaces after friction with Ni + 1×10^{17} B cm^{-2}, under a load of 2.5 N, a speed of 1.5 r.p.m., for 12 m. Pin: (a) back-scattered electrons, (b) Ni$K\alpha$ emission. Disc: (c) back-scattered electrons, (d) Fe$K\alpha$ emission.

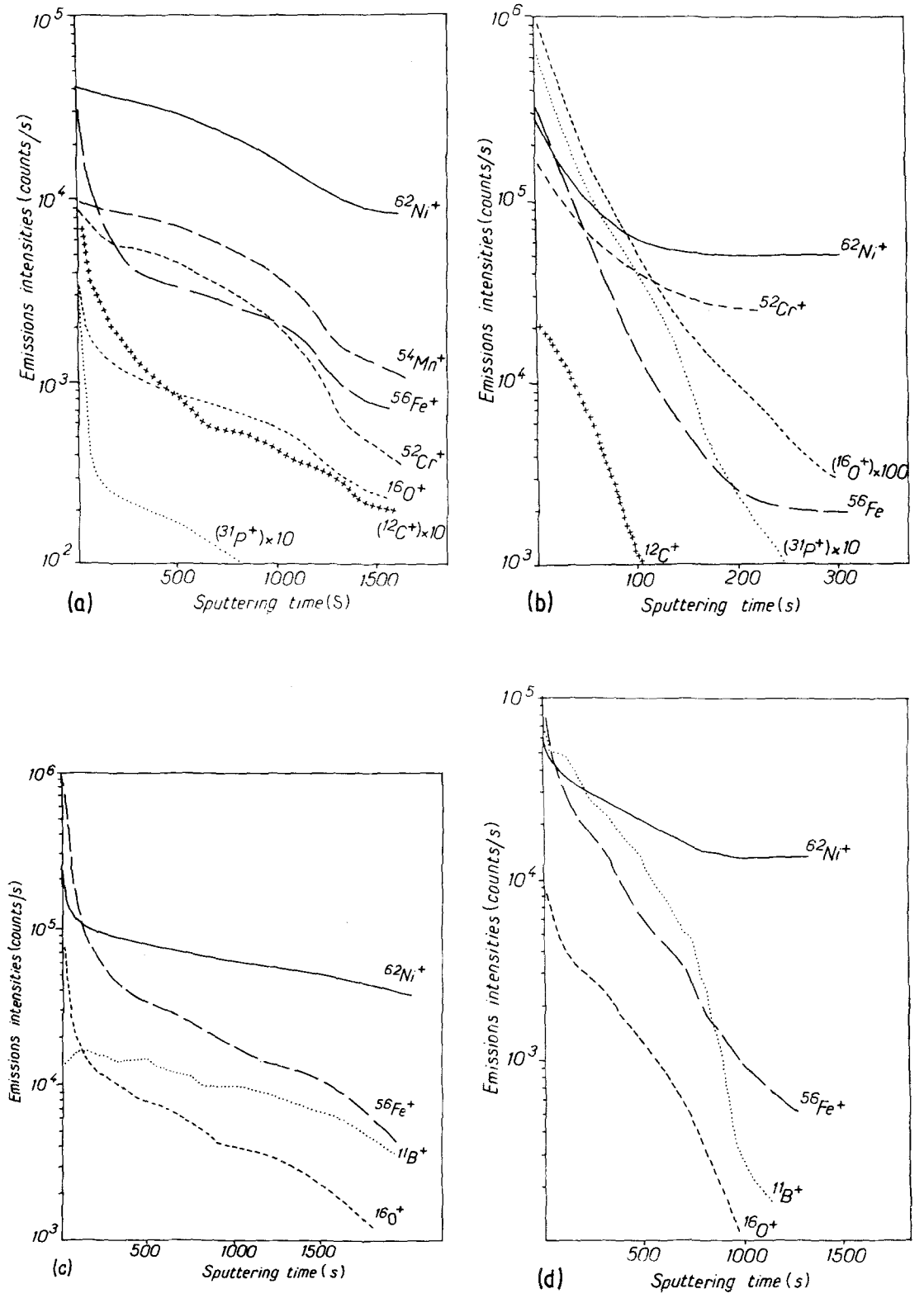

Figure 13 SIMS profiles recorded without oxygen flooding on surfaces worn under a load of 5 N at a speed of 1.5 r.p.m: (a) Ni + 5×10^{16} P cm^{-2} of energy 125 keV, sliding distance 7 m: (b) Ni + 2.5×10^{17} P cm^{-2} of 125 keV, 7 m; (c) Ni + 5×10^{16} B cm^{-2} of 50 keV, 12 m; (d) Ni + 2×10^{17} B cm^{-2} of 50 keV, 12 m.

TABLE IV

Implanted dose (ions cm^{-2})	Wear conditions			Residual dose (ions cm^{-2})	C^P or C^B (%) Depth (nm)			C^{Fe} (%) Depth (mn)		
	Load (N)	Speed (r.p.m.)	Sliding Distance (m)		0	100	500	0	100	500
5×10^{16} B	2.5	1.5	7	1.5×10^{14}	0.15	0.12	0.10	4.7	3.9	0.5
2×10^{17} B	5	1.5	12	3.7×10^{15}	0.12	0.07	0.01	1.4	1.5	1.6
2×10^{17} B	2.5	1.5	7	7.3×10^{16}	8.2	5.5	3.6	1.3	1.6	1.7
5×10^{16} P	2.5	1.5	7	2.5×10^{14}	0.24	0.04	0.04	1.9	1.4	1.3
2.5×10^{17} P	5	1.5	7	1.3×10^{17}	4.8	5.1	1.6	0.9	1.0	1.2
2.5×10^{17} P	2.5	1.5	7	2.3×10^{17}	8.2	2.4	0.16	0.8	0.8	1.0

removing 1 μm of the surface: the residual doses and concentrations of phosphorus and boron at several depths (0, 100 and 500 nm) are given in Table IV. The contents of iron, chromium, manganese, carbon and oxygen tend to decrease with the implanted dose.

4. Conclusion

The wear resistance of amorphous Ni–P or Ni–B implantation layers is much greater than that of pure nickel or of nickel surfaces implanted with intermediate doses, which remain crystalline, The amorphous surfaces are protected against seizure, which fact would account for a preponderant influence of the surface reactivity (adhesion) in our experiments.

The beneficial effect of boron or phosphorus implantation is perpetuated after removal of thickness of about 1 μm, i.e. considerably larger than the initial depth of implantation, because the implanted element diffuses during friction. But, this diffusion reflects also a local increase of temperature which could induce the crystallization of the surface. Indeed we were able to observe the superficial crystallization of Ni–B–Si melt-spun ribbons and also of Ni–B electroless deposits under less severe conditions of friction: during polishing of these surfaces with diamond and with lubrication. The crystallized layer could be removed by electrolytic dissolution of about 1 μm of surface [29].

Complementary experiments are necessary to obtain further insight in the comparison of superficial properties of amorphous and crystalline Ni–B or Ni–P surfaces. Experiments on hand are:

(a) the characterization of their mechanical properties by indentation to very shallow depths [30, 31].

(b) the characterization of their physico-chemical properties by MDS, UPS, XPS, ISS and SIMS analysis of adsorbed oxygen films, thermal oxide ones formed on as-implanted surfaces and of superficial changes of composition in worn surfaces [20];

(c) the characterization of the structure of worn surfaces by electron or X-ray diffraction at grazing incidence [29].

Finally it must be remembered that implanted surfaces are composite materials. The physico-chemical properties of Ni–B, NI–P implantation films are certainly similar to those of thicker electroless or electrochemical deposits, but their mechanical behaviour is more complex. Thus, reference will be made in further studies to the mechanical properties of Ni–B electroless deposits with various thicknesses in the range 1 to 20 μm [31].

Acknowledgements

Thanks are due to J. C. Chauveau, J. P. Champigny and D. L. Wehbi who programmed the processing of roughness measurements, to M. A. Clerc for the furnishing a Ni–B electroless coating, and to G. Lalu for ion implantations.

References

1. J. LOGAN and M. F. ASHBY, *Actal Metall.* **22** (1974) 1047.
2. T. MASUMOTO and R. MADDIN, *Mater. Sci. Eng.* **19** (1975) 1.
3. R. W. CAHN, *Ann. Rev. Mater. Sci.* **12** (1982) 57.
4. J. PEREZ, F. FOUQUET and G. LORMAND, Winterschool "Les Amorphes Métalliques", Aussois, France, 1983) (C.N.R.S., 15 Quai Anatole France, Paris, 1984).
5. D. H. BUCKLEY and K. MIYOSHI, Report of the National Aeronautics and Space Administration, Washington, DC 20546, NASA Technical Memo No. 82973 (1982) 25.
6. T. MASUMOTO and T. MURATA, *Mater. Sci. Eng.* **25** (1976) 71.
7. D. H. BUCKLEY and K. MIYOSHI, Report of the National Aeronautics and Space Administration,

Washington, DC 20546 Technical Memo No. 2140 (1983) 24.
8. J. K. A. AMUZU, *J. Phys. F.* **13** (1980) L127.
9. F. A. KUHNAST, F. MACHIZAUD, R. VANGELISTI and J. F. FLECHON, *J. Microsc. Spectrosc. Electron.* **5** (1980) 735.
10. G. EDELIN and C. TETE, *Scripta Metall.* **15** (1981) 739.
11. G. LINKER, *Nucl. Instrum. Meth.* **209–210** (1983) 969 and **182–183** (1981) 501.
12. G. CARTER and W. A. GRANT, *ibid.* **199** (1982) 17.
13. C. COHEN, A. V. DRIGO, H. BERNAS, J. CHAUMONT, K. KROLAS and L. THOME, *Phys. Rev. Lett.* **48** (1982) 1193.
14. L. THOME, J. C. PIVIN, A. BENYAGOUB, H. BERNAS and R. W. CAHN, *Ann. Chim. Fr.* **9** (1984) 287.
15. A. BENYAGOUB, H. BERNAS, J. CHAUMONT, L. THOME, C. COHEN and A. V. DRIGO, *Phys. Rev. B*, in press.
16. T. BARNAVON, Thesis, IPN Lyon, 69622 Villeurbanne, France (1982).
17. N. E. W. HARTLEY, W. E. SWINKLEHURST, G. DEARNALEY and J. F. TURNER, *J. Mater. Sci.* **8** (1973) 900.
18. H. HERMAN, *Nucl. Instrum. Meth.* **182–183** (1981) 887.
19. I. L. SINGER, C. A. CAROSELLA and J. R. REED, *ibid.* **182–183** (1981) 923.
20. J. C. PIVIN, J. PERREAU, C. REYNAUD, J. TAKADOUM and C. BOIZIAN, *Phys. Rev. B*, submitted for publication.
21. J. CHAUMONT, F. LALU, M. SALOME, A. M LAMOISE and H. BERNAS, *Nucl. Instrum. Meth.* **189** (1981) 193.
22. J. TAKADOUM, J. C. PIVIN, J. PONS–CORBEAU, R. BERNERON and J. C. CHARBONNIER, *Surf. Interf. Anal.* **6** (1984) 174.
23. G. TOURLONIAS, INSA, Lyon, France.
24. T. R. THOMAS, *Wear* **33** (1975) 205.
25. D. WEHBI and C. ROQUES–CARMES, Proceedings of the Tenth International Conference on X-ray Optics and Microanalysis, J. Phys. Coll. C2, Suppl. 2 **45** (1984) 319.
26. G. SLODZIAN, *Ann. Phys.* **9** (1974) 591.
27. J. C. PIVIN and C. ROQUES–CARMES, *J. Microsc. Spectrosc. Electron.* **7** (1982) 277.
28. D. LEBOUVIER, Microthesis, C.E.M.E.F., Vallebonne, 06560 France (1983).
29. C. ROQUES–D. MAIREY and J. C. PIVIN, Courrier de la Société Française de Tribologie, Paris, France, March (1984).
30. D. NEWEY, M. A. WALKINS and H. M. POLLOCK, *J. Phys. E: Sci. Instrum.* **15** (1982) 119.
31. J. TAKADOUM, J. C. PIVIN, J. RUSS, H. M. POLLOCK and H. BERNAS, *Nucl. Instrum. Methods*, submitted for publication.

Received 19 March
and accepted 12 April 1984